Solvent Dependence of Charge Separation and Charge Recombination Rates in Porphyrin−Fullerene Dyad

Hiroshi Imahori,* Mohamed E. El-Khouly,† Mamoru Fujitsuka,† Osamu Ito,†,* Yoshiteru Sakata,‡ and Shunichi Fukuzumi*

Department of Material and Life Science, Graduate School of Engineering, Osaka University, CREST, Japan Science and Technology Corporation, Suita, Osaka 565-0871, Japan, Institute for Chemical Reaction Science, Tohoku University, Katahira, Aoba-ku, Sendai 980-8577, Japan, and The Institute of Scientific and Industrial Research, Osaka University, 8-1 Mihoga-oka, Ibaraki, Osaka 567-0047, Japan

Received: June 15, 2000; In Final Form: October 27, 2000

Photoinduced processes in zinc porphyrin−C_{60} dyad (ZnP−C_{60}) in different organic solvents have been investigated by fluorescence lifetime measurements and pico- and nanosecond time-resolved transient absorption spectroscopies. Irrespective of the solvent polarity, the charge-separated state ($ZnP^{\bullet+}-C_{60}^{\bullet-}$) is formed via photoinduced electron transfer from the excited singlet state of the porphyrin to the C_{60} moiety. However, the resulting charge-separated state decays to different energy states depending on the energy level of the charge-separated state relative to the singlet and triplet excited states of the C_{60} moiety. In nonpolar solvents such as benzene ($\epsilon_s = 2.28$), the charge-separated state undergoes charge recombination to yield the C_{60} singlet excited state, followed by intersystem crossing to the C_{60} triplet excited state, since the energy level of the charge-separated state is higher than that of the C_{60} singlet excited state (1.75 eV). More polar solvents such as anisole ($\epsilon_s = 4.33$) render the energy level of the charge-separated state lower than the C_{60} singlet excited state, resulting in the direct formation of the C_{60} triplet excited state (1.50 eV) from the charge-separated state, formed by the photoinduced charge separation from the porphyrin to the C_{60} singlet excited state as well as from the porphyrin excited singlet state to the C_{60}. In polar solvents such as benzonitrile ($\epsilon_s = 25.2$), where the energy level of the charge-separated state (1.38 eV) is low compared with the C_{60} triplet excited state, the charge-separated state, produced upon excitation of the both chromophores, decays directly to the ground state. Such solvent dependence of charge recombination processes in ZnP−C_{60} can be rationalized by small reorganization energies of porphyrins and fullerenes in electron-transfer processes.

Introduction

Excited-state properties and photoinduced electron transfer (ET) reactions of covalently linked donor−acceptor systems have been extensively studied to mimic photosynthetic ET.[1] The fundamental strategy in mimicking photosynthesis involves application of multistep ET and control of reorganization energy (λ).[2] In particular, it seems of fundamental significance to achieve small reorganization energy in ET systems, since the charge recombination (CR) processes can be markedly decelerated by shifting the energetics deep into the Marcus inverted region, where the driving force ($-\Delta G^0_{et}$) is larger than the reorganization energy of ET.[3] In this context, utilization of fullerenes as an electron acceptor has been demonstrated to be very effective,[4] because of the small reorganization energies of fullerenes in ET.[5] The most extensively studied fullerene-based systems are porphyrin-linked fullerenes,[5−15] where a porphyrin is used as an electron donor as well as a sensitizer. In these studies, both photoinduced energy transfer (EN) and ET have been reported to occur. It is well established for porphyrin−C_{60} systems that the charge-separated state is formed in polar solvents via photoinduced ET.[5−15] Although some systems have been reported to produce the charge-separated states even in nonpolar solvents,[5a−c,6e,8c,9b,11,13c] most other systems have exhibited direct singlet−singlet EN from the porphyrin to the fullerene moiety in nonpolar solvents such as toluene ($\epsilon_s = 2.38$) and benzene ($\epsilon_s = 2.28$). Thus, a systematic study on the solvent-dependent change in the charge separation (CS) and CR processes in porphyrin−fullerene linked systems has yet to be reported.

This study reports detailed solvent dependence of both CS and CR processes in porphyrin−C_{60} dyad (ZnP−C_{60}) (Figure 1). A porphyrin is connected to C_{60}, with a relatively rigid spacer [the edge-to-edge distance (R_{ee}) = 11.9 Å and the center-to-center distance (R_{cc}) = 18.0 Å] so that the photodynamics can be analyzed at a fixed distance between the porphyrin and C_{60} moieties. The photodynamical processes have been studied by fluorescence lifetime measurements and pico- and nanosecond laser flash photolysis. These flash photolysis experiments will reveal the spectral characteristics of the zinc porphyrin radical cation ($ZnP^{\bullet+}$) and the C_{60} radical anion ($C_{60}^{\bullet-}$) moieties in the charge-separated state in benzene, anisole, and benzonitrile. In addition, the C_{60} and porphyrin triplet excited states can be monitored by nanosecond flash photolysis. Complementary information on the excited singlet states of the porphyrin and the C_{60} will be provided by the fluorescence lifetime experiments.

* Authors for correspondence. E-mail: imahori@ap.chem.eng.osaka-u.ac.jp, ito@icrs.tohoku.ac.jp, fukuzumi@ap.chem.eng.osaka-u.ac.jp.
† Institute for Chemical Reaction Science.
‡ Institute of Scientific and Industrial Research.

10.1021/jp002158b CCC: $20.00
Published on Web 12/20/2000

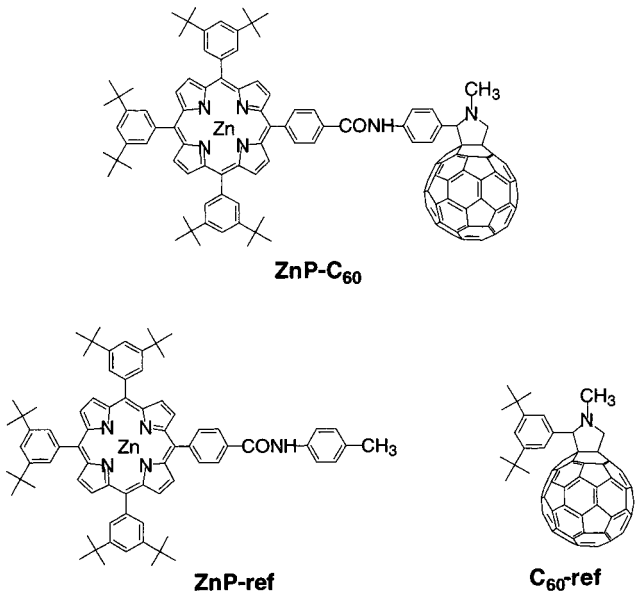

Figure 1. Structures of molecules.

Experimental Section

Materials. ZnP−C_{60}[15] was obtained by 1,3-dipolar cycloaddition using the corresponding porphyrin aldehyde.[16] Porphyrin reference (ZnP−ref) was prepared by the coupling reaction of 5-(4-carboxyphenyl)-10,15,20-tris(3,5-di-*tert*-butylphenyl)porphyrin and 4-methylaniline, followed by treatment with Zn(OAc)$_2$. C_{60} reference (C_{60}−ref[13f]) was synthesized from 3,5-di-*tert*-butylbenzaldehyde, *N*-methylglycine, and C_{60} by the same method as described for ZnP−C_{60}.

Structures of all new compounds were confirmed by spectroscopic analysis including ^{1}H NMR, infrared (IR), and fast atom bombardment (FAB) mass spectra.[15] Tetrabutylammonium hexafluorophosphate used as a supporting electrolyte for the electrochemical measurements was obtained from Tokyo Kasei Organic Chemicals. Benzene, anisole, and benzonitrile were purchased from Wako Pure Chemical Ind., and purified by successive distillation over calcium hydride.

ZnP−Ref. A solution of 5-(4-carboxyphenyl)-10,15,20-tris(3,5-di-*tert*-butylphenyl)porphyrin[15] (200 mg, 0.207 mmol), pyridine (0.33 mL, 4.32 mmol), and thionyl chloride (0.095 mL, 0.648 mmol) in benzene (30 mL) was refluxed for 1 h. The excess thionyl chloride and solvents were removed under reduced pressure and the residue was redissolved in benzene (20 mL). This solution was added to a stirred solution of 4-methylaniline (23.0 mg, 0.215 mmol) in benzene (10 mL) and pyridine (1 mL), and the solution was stirred for 12 h. The solvent was removed under reduced pressure. Flash column chromatography on silica gel with benzene (R_f = 0.35) as an eluent and subsequent reprecipitation from benzene−acetonitrile gave a vivid reddish-purple solid. A saturated methanol solution of Zn(OAc)$_2$ (3 mL) was added to a solution of the resultant solid in $CHCl_3$ (30 mL) and refluxed for 30 min. After cooling, the reaction mixture was washed with water twice, dried over anhydrous Na_2SO_4, and then the solvent was evaporated. Flash column chromatography on silica gel with benzene (R_f = 0.30) as an eluent and subsequent reprecipitation from benzene−acetonitrile gave ZnP−ref as a deep red-purple solid (72% yield, 171 mg, 0.149 mmol); mp > 300 °C; ^{1}H NMR (270 MHz, $CDCl_3$) δ 9.02 (d, J = 5 Hz, 2H), 9.01 (s, 4H), 8.90 (d, J = 5 Hz, 2H), 8.37 (d, J = 8 Hz, 2H), 8.22 (d, J = 8 Hz, 2H), 8.09 (m, 7H), 7.79 (m, 3H), 7.66 (d, J = 8 Hz, 2H), 7.27 (d, J = 8 Hz, 2H), 2.40 (s, 3H), 1.53 (s, 54H); mass spectrometry (FAB) 1146 (M + H$^+$); Fourier transform IR (KBr) 3059, 2962, 2905, 2869, 2364, 2345, 1804, 1686, 1658, 1593, 1519, 1493, 1477, 1425, 1406, 1398, 1363, 1340, 1316, 1290, 1247, 1219, 1205, 1069, 1001, 947, 930, 899, 883, 823, 797, 759, 745, 718, 508 cm^{-1}.

Spectral Measurements. Time-resolved fluorescence spectra were measured by a single-photon counting method using a second harmonic generation (SHG, 410 nm) of a Ti:sapphire laser [Spectra-Physics, Tsunami 3950-L2S, 1.5 ps full width at half-maximum (fwhm)] and a streakscope (Hamamatsu Photonics, C4334-01) equipped with a polychromator (Acton Research, SpectraPro 150) as an excitation source and a detector, respectively.

Picosecond laser flash photolysis was carried out using SHG (532 nm) of active/passive mode-locked Nd:YAG laser (Continuum, PY61C-10, fwhm 35 ps) as the excitation light. A white continuum pulse generated by focusing the fundamental of the Nd:YAG laser on a D_2O/H_2O (1:1 volume) cell was used as monitoring light. The visible monitoring light transmitted through the sample was detected with a dual MOS detector (Hamamatsu Photonics, C6140) equipped with a polychromator (Acton Research, SpectraPro 150). For detection of the near-IR light, an InGaAs linear image sensor (Hamamatsu Photonics, C5890−128) was used as a detector. The spectra were obtained by averaging 80 events on a microcomputer. The time resolution of the present system was ca. 35 ps.

Nanosecond transient absorption measurements were carried out using SHG (532 nm) of Nd:YAG laser (Spectra-Physics, Quanta-Ray GCR-130, fwhm 6 ns) as an excitation source. For transient absorption spectra in the near-IR region (600−1600 nm), monitoring light from a pulsed Xe lamp was detected with a Ge-avalanche photodiode (Hamamatsu Photonics, B2834). Photoinduced events in micro- and millisecond time regions were estimated by using a continuous Xe lamp (150 W) and an InGaAs−PIN photodiode (Hamamatsu Photonics, G5125−10) as a probe light and a detector, respectively. Details of the transient absorption measurements were described elsewhere.[17] All the samples in a quartz cell (1 × 1 cm) were deaerated by bubbling argon through the solution for 15 min.

Steady-state absorption spectra in the visible and near-IR regions were measured on a Jasco V570 DS spectrophotometer. Fluorescence spectra were measured on Hitachi 850 spectrofluorophotometer.

Electrochemical Measurements. The cyclic voltammetry measurements were performed on a BAS 50 W electrochemical analyzer in deaerated benzonitrile solution containing 0.10 M Bu_4NPF_6 as a supporting electrolyte at 298 K (100 mV s^{-1}). The glassy carbon working electrode was polished with BAS polishing alumina suspension and rinsed with acetone before use. The counterelectrode was a platinum wire. The measured potentials were recorded with respect to an Ag/AgCl (saturated KCl) reference electrode.

Results and Discussion

Steady-State Absorption and Fluorescence Studies. Figure 2 shows absorption spectra of ZnP−C_{60} and the references (ZnP−ref and C_{60}−ref) in benzonitrile. The absorption spectrum of ZnP−C_{60} in benzonitrile is virtually the superposition of the spectra of the individual chromophores, indicating that there is no evidence for strong interaction between the chromophores in the ground state. Similar results were obtained in benzene and anisole.

Steady-state fluorescence spectra of ZnP−C_{60} and the references (ZnP−ref and C_{60}−ref) were measured in benzene,

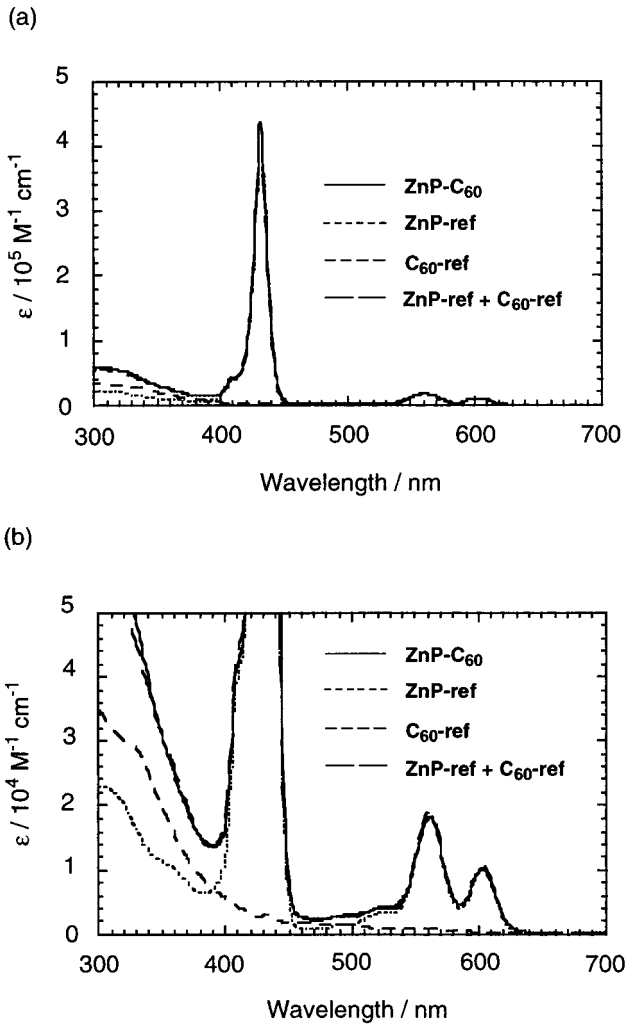

Figure 2. (a) Absorption spectra of ZnP−C_{60} (solid line), ZnP−ref (dotted line), and C_{60}−ref (dashed line) in benzonitrile. (b) Spectra are expanded by a factor of 10 along vertical axis. Spectrum of a superposition of ZnP−ref and C_{60}−ref (broken line) is shown for comparison.

anisole, and benzonitrile with excitation at 410 nm, where the absorption ratios of the porphyrin and C_{60} moieties are 92:8 in benzene and 90:10 in anisole and benzonitrile. A typical example in benzene is shown in Figure 3. Emissions from both the porphyrin moiety (λ_{max} = 600, 645 nm)[5a−c,13] and the C_{60} moiety (λ_{max} = 710 nm)[5a−c,13] are clearly observed for ZnP−C_{60} in benzene, anisole, and benzonitrile. However, the fluorescence spectra of ZnP−C_{60} are quenched more strongly than those of ZnP−ref under the same conditions (relative intensity = 0.027), indicating that ^{1}ZnP* is quenched by the C_{60} moiety. It is interesting to note that the emission intensity of the C_{60} moiety relative to the porphyrin decreases with increasing solvent polarity.

Fluorescence Lifetime Measurements. The fluorescence lifetimes (τ) of ZnP−C_{60}, ZnP−ref, and C_{60}−ref were measured by a time-correlated single-photon-counting apparatus with excitation at 410 nm, and monitored at 610 and 720 nm, where the emission is due to the porphyrin and the C_{60} moiety, respectively. The results are summarized in Table 1. The fluorescence decay curve was well fitted as a single exponential. The fluorescence lifetimes of ZnP−C_{60} at 610 nm [τ = 100 ps (benzonitrile), 120 ps (anisole), 200 ps (benzene)] are much shorter than those of ZnP−ref (2000−2100 ps). This indicates that the rapid quenching of the porphyrin singlet excited state

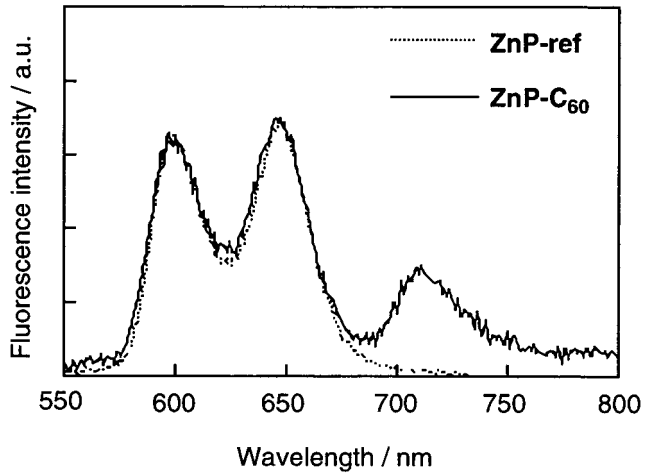

Figure 3. Steady-state fluorescence spectra of ZnP−C_{60} (solid line) and ZnP−ref (dotted line) in benzene (λ_{ex} = 410 nm, absorption ratio of ZnP:C_{60} = 92:8). The spectra are normalized at the peak position for comparison.

TABLE 1: Fluorescence Lifetimes (τ) of ZnP−C_{60} and the Reference Compounds in Benzene, Anisole, and Benzonitrile[a]

	lifetime (τ)/ps					
	benzene (ϵ_s = 2.28)		anisole (ϵ_s = 4.33)		benzonitrile (ϵ_s = 25.2)	
compound λ_{obs}	610 nm	720 nm	610 nm	720 nm	610 nm	720 nm
ZnP−C_{60}	200	1200	120	1100	100	760
ZnP−ref	2000		2100		2000	
C_{60}−ref		1300		1300		1300

[a] Absorption ratio of ZnP and C_{60} in ZnP−C_{60} at excitation wavelength (λ_{ex} = 410 nm); ZnP:C_{60} = 92:8 (benzene), 90:10 (anisole and benzonitrile).

(^{1}ZnP*) occurs by the attached C_{60} moiety through ET or EN or both, judging from the results reported for zinc porphyrin−C_{60} dyads.[5−15] On the other hand, the fluorescence lifetimes of ZnP−C_{60} at 720 nm [τ = 760 ps (benzonitrile), 1100 ps (anisole), 1200 ps (benzene)] become longer as the solvent polarity decreases, approaching the lifetime of C_{60}−ref (1300 ps). This suggests that the excited singlet state of the C_{60} ($^1C_{60}$*) is less quenched by the attached porphyrin in nonpolar solvents through ET, which will be discussed in a later section. It should be noted here that a rise component of the fluorescence at 750 nm with a rate constant of 2.5 × 10^9 s^{-1}, where the emission is due to the C_{60} solely, was clearly detected in benzene, as shown in Figure 4. This is in sharp contrast with no appearance of the fluorescence rise in anisole and benzonitrile. Because the rise rate (rate constant of 2.5 × 10^9 s^{-1}) at 750 nm due to $^1C_{60}$* in benzene does not match the decay rate (rate constant of 5.0 × 10^9 s^{-1}) at 610 nm due to ^{1}ZnP*, it is strongly suggested that the charge-separated state (ZnP$^{\bullet+}$−$C_{60}^{\bullet-}$) in benzene, produced via photoinduced ET, undergoes the CR to yield $^1C_{60}$*. Such recombination of charge-separated state (ZnP$^{\bullet+}$-$C_{60}^{\bullet-}$) to $^1C_{60}$* has also been reported in porphyrin−C_{60} dyads.[5a−c,6e,13c]

Time-Resolved Transient Absorption Spectra. Time-resolved transient absorption spectra of ZnP−C_{60} in various solvents were measured by pico- and nanosecond laser photolysis with excitation wavelength at 532 nm, where the absorption ratios of the porphyrin and the C_{60} moieties are 85:15 in benzene, 76:24 in anisole, and 77:23 in benzonitrile. Figure 5 displays picosecond time-resolved absorption spectra of ZnP−C_{60} in benzene. The $S_n \leftarrow S_1$ difference spectrum taken immediately after excitation with 532-nm laser pulse (50-ps

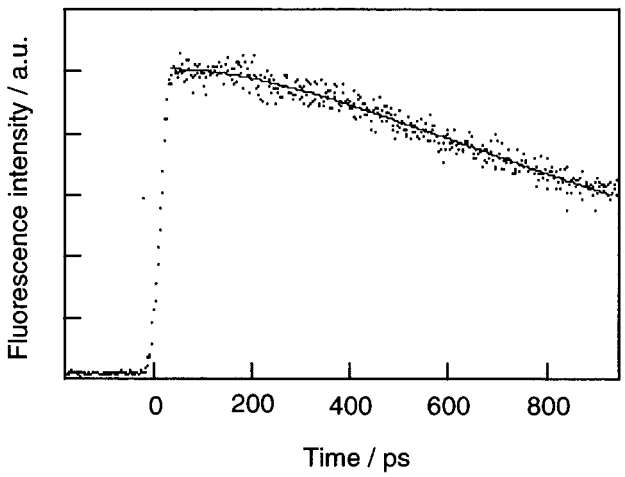

Figure 4. Time profiles of fluorescence intensity for ZnP−C_{60} in argon-saturated benzene monitored at 750 nm (λ_{ex} = 410 nm). The time profile was fitted by rise (rate constant of 2.5×10^9 s^{-1}) and decay (rate constant of 7.7×10^8 s^{-1}) components, respectively.

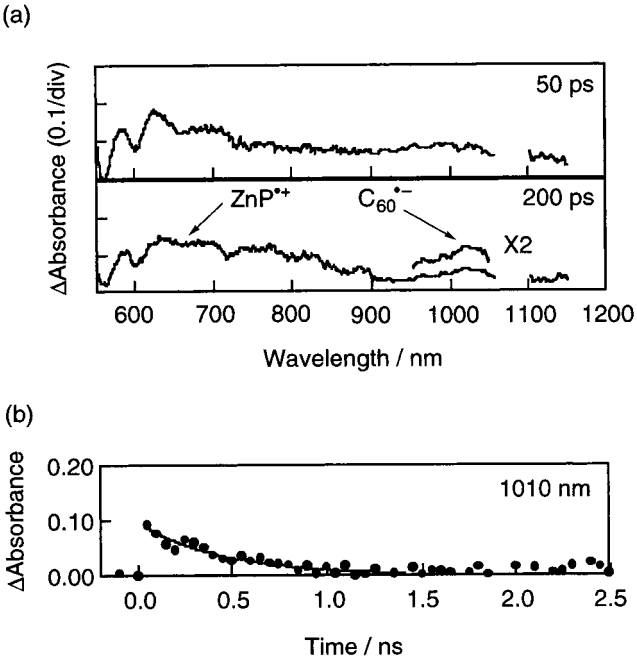

Figure 5. (a) Picosecond time-resolved absorption spectra of ZnP−C_{60} in argon-saturated benzene excited at 532 nm (absorption ratio of ZnP:C_{60} = 85:15) and (b) time dependence of the absorbance at 1010 nm. The solid line shows a simulated curve using a rate constant of 2.5×10^9 s^{-1}.

delay) is characterized by the bleaching of the ground-state porphyrin absorption at 560 and 600 nm of the Q-bands, the stimulating emission from the porphyrin at 650 nm, and the broad absorption of $^1C_{60}$* at near-IR region. With increasing delay time (200-ps delay), a new absorption band at 1020 nm due to the C_{60} radical anion ($C_{60}^{\bullet-}$)[15,18] appears clearly, accompanied by the rise in a broad absorption around 650 nm due to zinc porphyrin radical cation ($ZnP^{\bullet+}$).[13c,19] These results clearly show that photoinduced ET takes place from ^{1}ZnP* to C_{60} in ZnP−C_{60}, resulting in formation of the charge-separated state. On the basis of the fluorescence lifetimes, the CS rate (k_{CS1}) from ^{1}ZnP* and the quantum yield (Φ) of formation of the charge-separated state were estimated as 4.5×10^9 s^{-1} and 0.90, respectively (Table 2). Similar transient absorption spectra, exhibiting the formation of $ZnP^{\bullet+}$ and $C_{60}^{\bullet-}$, were obtained in anisole and benzonitrile. The values of ET rates and quantum yields are summarized in Table 2. The CS rates from ^{1}ZnP* to C_{60} in ZnP−C_{60} are nearly the same in benzene, anisole, and benzonitrile. This may result from an increase in both the reorganization energy and driving force for CS with increasing solvent polarity, leading to similar CS irrespective of the solvent polarity.[5a,13c] The decay profile at 1010 nm in benzene was analyzed by a single exponential with a rate constant of 2.5×10^9 s^{-1}, as shown in Figure 5b. The time constant ($k_{CR2} = 2.5 \times 10^9$ s^{-1}) agrees well with that of the fluorescence rise from the C_{60} moiety at 750 nm (2.5×10^9 s^{-1}) (Figure 4).

The energy level of the charge-separated state is known to be pushed up in nonpolar solvents such as benzene (ϵ_s = 2.28) and toluene (ϵ_s = 2.38), as compared with polar solvents. Thus, the charge-separated state ($ZnP^{\bullet+}-C_{60}^{\bullet-}$) is located between ^{1}ZnP* (2.08 eV) and $^1C_{60}$* (1.75 eV) in benzene, as illustrated in Scheme 1.[5a,13c] This is consistent with the fact that $^1C_{60}$* is

TABLE 2: CS and CR Rate Constants in ZnP−C_{60}

solvent	initial state	final state	$-\Delta G^0_{ET}$/ eV[a]	k_{ET}/ s^{-1} [b]	Φ[c]
benzene	^{1}ZnP*	$ZnP^{\bullet+}-C_{60}^{\bullet-}$	<0.33	4.5×10^9	0.90
(ϵ_s = 2.28)	$ZnP^{\bullet+}-C_{60}^{\bullet-}$	$^1C_{60}$*	<0.33	2.5×10^9	~1
anisole	^{1}ZnP*	$ZnP^{\bullet+}-C_{60}^{\bullet-}$	0.32−0.57	7.8×10^9	0.94
(ϵ_s = 4.33)	$^1C_{60}$*	$ZnP^{\bullet+}-C_{60}^{\bullet-}$	<0.25	1.4×10^8	0.15
	$ZnP^{\bullet+}-C_{60}^{\bullet-}$	$^3C_{60}$*	<0.25	3.0×10^8	~1[d]
benzonitrile	^{1}ZnP*	$ZnP^{\bullet+}-C_{60}^{\bullet-}$	0.66	9.5×10^9	0.95
(ϵ_s = 25.2)	$^1C_{60}$*	$ZnP^{\bullet+}-C_{60}^{\bullet-}$	0.37	5.5×10^8	0.42
	$^3C_{60}$*	$ZnP^{\bullet+}-C_{60}^{\bullet-}$	0.12	1.5×10^7	0.99
	$ZnP^{\bullet+}-C_{60}^{\bullet-}$	ZnP−C_{60}	1.38	1.3×10^6	1

[a] $-\Delta G^0_{CR} = E^0_{ox}$ (D/$D^{\bullet+}$) − E^0_{red} (A/$A^{\bullet-}$), $-\Delta G^0_{CS} = \Delta E_{0-0} - (-\Delta G^0_{CR})$, where E^0_{ox} (D/$D^{\bullet+}$) and E^0_{red} (A/$A^{\bullet-}$) are the first oxidation potential of donor and the first reduction potential of acceptor, respectively, and ΔE_{0-0} is energy of the 0−0 transition between the lowest excited state and the ground state. The redox potentials were measured by differential pulse voltammetry in benzonitrile using 0.1 M Bu_4NPF_6 as supporting electrolyte. The Coulombic term in polar solvents such as benzonitrile is negligible. On the other hand, in nonpolar solvents such as anisole and benzene it was impossible to determine $-\Delta G^0_{ET}$ with accuracy, because of the difficulty in estimating the Coulombic term and the redox potentials in nonpolar solvents. [b] Charge separation (CS) rates from ^{1}ZnP* and $^1C_{60}$* were determined from the following equation using the fluorescence lifetimes: $k_{CS} = [1/\tau\ (ZnP-C_{60})] - [1/\tau\ (ZnP-ref\ or\ C_{60}-ref)]$. The other CS and charge recombination rates were determined by analyzing the rise or decay of $C_{60}^{\bullet-}$ at 1000−1010 nm. [c] The quantum yields (Φ) for each pathway were estimated on a basis of Schemes 1−3. [d] Assuming that contribution of the deactivation pathway from $ZnP^{\bullet+}-C_{60}^{\bullet-}$ to ^{3}ZnP* (1.53 eV)[15] is negligible.

SCHEME 1: Schematic Energy Levels and Relaxation Pathways for ^{1}ZnP* and $^1C_{60}$* in ZnP−C_{60} in Benzene; $k_0 = 5.0 \times 10^8$ s^{-1}, $k_{CS1} = 4.5 \times 10^9$ s^{-1}, $k_{CR1} < 1.3 \times 10^6$ s^{-1}, $k_{CR2} = 2.5 \times 10^9$ s^{-1}, $k_{ISC} = 7.7 \times 10^8$ s^{-1}, $k_T = 2.2 \times 10^5$ s^{-1}

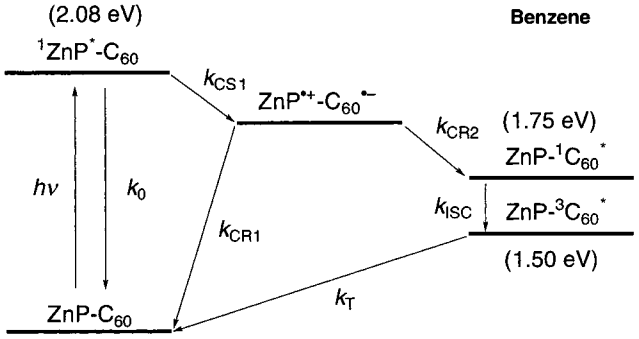

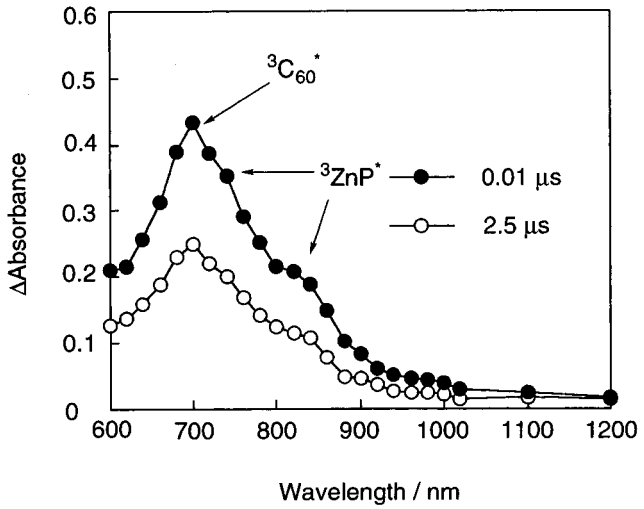

Figure 6. Nanosecond transient absorption spectra obtained by 532-nm (absorption ratio of ZnP:C_{60} = 85:15) laser photolysis of ZnP−C_{60} (0.1 mM) in argon-saturated benzene.

almost unquenched by ZnP in ZnP−C_{60} (Table 1). The distinctobservation of the charge-separated state in both nonpolar and polar solvents contrasts with previous reports that efficient singlet−singlet EN from porphyrin to C_{60} occurs in nonpolar solvents such as benzene and toluene.[6a−c,7,10c,11] It is well established that *intramolecular* EN rates are not susceptible to solvent polarity.[20] If the EN process occurs with a rate constant of $\sim 10^{10}$ s^{-1} in nonpolar solvents, the EN process with the similar rate constant would be observed in polar solvents as well. However, no observation of such EN process in polar solvents precludes such possibility. Because CR rates in donor−acceptor linked dyads are known to decrease with decreasing solvent polarity,[21] the CR rate (k_{CR1}) from the charge-separated state to the ground state in nonpolar solvents would be slower than the CR rate (1.3×10^6 s^{-1}) in benzonitrile (vide infra, see Table 2). Therefore, the quantum yield of formation of $^1C_{60}$* from the charge-separated state in benzene can be estimated as almost unity (∼1). The reorganization energies of porphyrin−fullerene systems are known to be small,[5] and driving force for the CR to the ground state (>1.75 eV) is much larger than that for the CR to the $^1C_{60}$* (<0.33 eV). Thus, the driving force for the CR to $^1C_{60}$* is located in the normal or top region of the Marcus parabola, whereas the driving force for the CR to the ground state goes deep into the Marcus inverted region. Consequently, the CR to$^1C_{60}$* in benzene is dominant over the CR to the ground state.

Formation of the C_{60} triplet excited state ($^3C_{60}$*) in argon-saturated benzene is also confirmed by the complementary nanosecond experiments, as shown in Figure 6, which exhibits a characteristic triplet−triplet absorption maximum at 700 nm. In addition, the weak transient absorption due to the porphyrin triplet excited state (^{3}ZnP*) appears at 740 and 840 nm.[15,22] The ^{3}ZnP* (1.53 eV)[15] may be produced from the intersystem crossing from ^{1}ZnP* in ZnP−C_{60}. Considering the molar absorption coefficient of $^3C_{60}$* (ϵ = 4200 M^{-1} cm^{-1})[23] and ^{3}ZnP* (ϵ = 8500 M^{-1} cm^{-1}),[22] it is concluded that the $^3C_{60}$* is generated predominately via the intersystem crossing from $^1C_{60}$* with a rate constant of 7.7×10^8 s^{-1} (Scheme 1).[15] The resulting $^3C_{60}$* decays to the ground state with a rate constant of 2.2×10^5 s^{-1}.

In anisole, photoinduced ET also occurs from ^{1}ZnP* to C_{60} to yield the charge-separated state with a rate constant of 7.8×10^9 s^{-1} and the quantum yield of 0.94, which are obtained

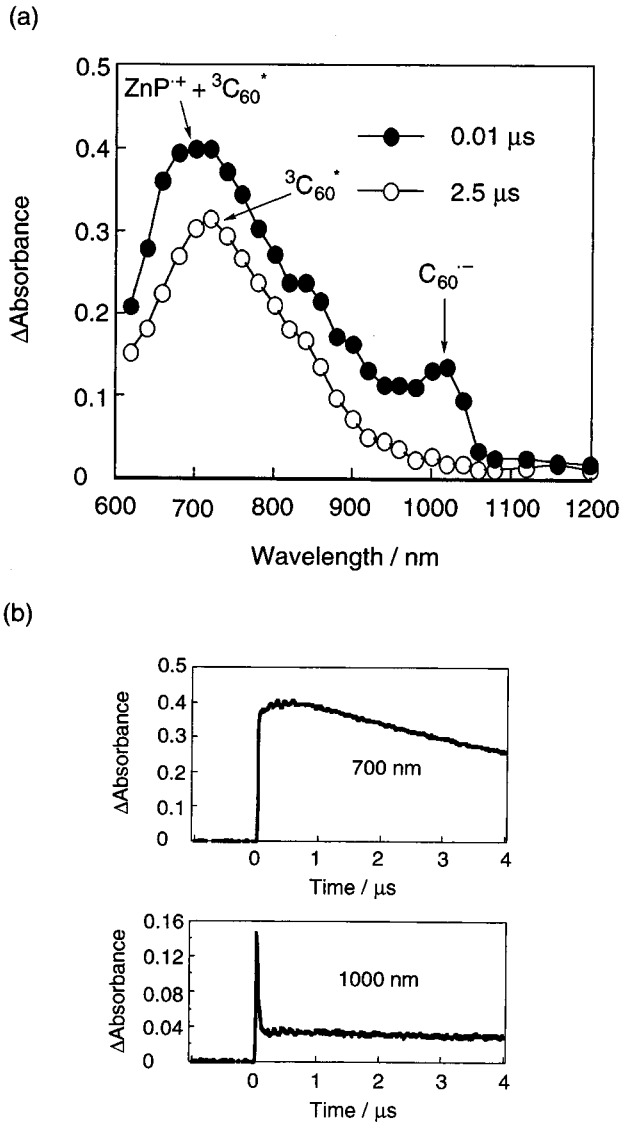

Figure 7. (a) Nanosecond time-resolved absorption spectra obtained by 532-nm (absorption ratio of ZnP:C_{60} = 76:24) laser photolysis of ZnP−C_{60} (0.1 mM) in argon-saturated anisole and (b) time profiles of absorbance at 700 and 1000 nm.

using the fluorescence lifetimes (Table 2). However, with increasing the solvent polarity from benzene (ϵ_s = 2.28) to anisole (ϵ_s = 4.33), the deactivation pathway from the charge-separated state changes drastically. Figure 7a shows nanosecond time-resolved transient absorption spectra of ZnP−C_{60} in anisole. Both transient absorption bands due to $^3C_{60}$* (λ_{max} = 700 nm) and $C_{60}^{\bullet-}$ (λ_{max} = 1020 nm) appear within the time resolution (10 ns). The unambiguous detection of ^{3}ZnP* was somewhat obscured in anisole, since the absorption due to ^{3}ZnP* overlaps with the $^3C_{60}$* absorption extensively at 600−900 nm. However, the contribution of ^{3}ZnP*, if any, would be minor, as is the case in benzene (Figure 6). The absorption band at 1020 nm due to $C_{60}^{\bullet-}$ decays rapidly to leave the characteristic band at 700 nm due to the $^3C_{60}$* (Figure 7b). The decay rate (k_{CR2}) at 1020 nm was determined as 3.0×10^8 s^{-1} using picosecond transient absorption spectroscopy (Table 2). Because no rise component due to the formation of $^1C_{60}$* was observed in the fluorescence lifetime measurement in anisole, the $ZnP^{\bullet+}$−$C_{60}^{\bullet-}$ state recombines to generate $^3C_{60}$* in anisole, as illustrated in Scheme 2. The quantum yield of formation of $^3C_{60}$* from the charge-separated state can be estimated as almost unity (∼1),

SCHEME 2: Schematic Energy Levels and Relaxation Pathways for ^{1}ZnP* and $^1C_{60}$* in ZnP−C_{60} in Anisole; $k_0 = 4.8 \times 10^8$ s^{-1}, $k_{CS1} = 7.8 \times 10^9$ s^{-1}, $k_{CS2} = 1.4 \times 10^8$ s^{-1}, $k_{CR1} < 1.3 \times 10^6$ s^{-1}, $k_{CR2} = 3.0 \times 10^8$ s^{-1}, $k_{ISC} = 7.7 \times 10^8$ s^{-1}, $k_T = 1.2 \times 10^5$ s^{-1}

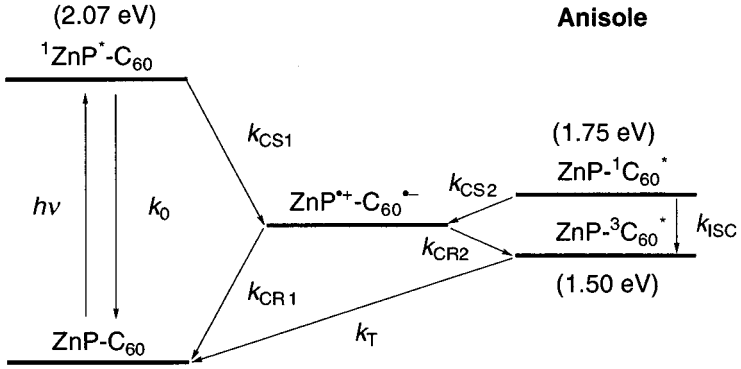

because the CR to the ground state ($<1.3 \times 10^6$ s^{-1}) is much slower than the CR to the $^3C_{60}$* (3.0×10^8 s^{-1}). Judging from the fact that the driving force for the former (>1.50 eV) is much larger than that for the latter (<0.25 eV), the CR processes to the ground state and to the $^3C_{60}$* are located in the Marcus inverted region and normal region, respectively. Accordingly, the preference for the latter process over the former one may be explained by the small reorganization energy (<0.8 eV in anisole) of porphyrin−C_{60} linked systems (vide supra). It is interesting to note that the charge-separated state is likely to yield $^3C_{60}$* (1.50 eV) rather than ^{3}ZnP* (1.53 eV) in anisole. The predominant formation of the $^3C_{60}$* over ^{3}ZnP* may be accommodated by smaller reorganization energy of the C_{60} over the porphyrin, in addition to the slightly larger driving force for the former (<0.25 eV) against the latter (<0.22 eV) in the Marcus normal region. The resulting $^3C_{60}$*, generated from both the ZnP$^{\bullet+}$−$C_{60}^{\bullet-}$ state and $^1C_{60}$* ($k_{ISC} = 7.7 \times 10^8$ s^{-1}), decays to the ground state with a rate constant (k_T) of 1.2×10^5 s^{-1} at 700 nm (Scheme 2). The rate constant ($k_{CR2} = 3.0 \times 10^8$ s^{-1}) in anisole is one order of magnitude smaller than k_{CR2} (2.5×10^9 s^{-1}) for CR from ZnP$^{\bullet+}$−$C_{60}^{\bullet-}$ to the $^1C_{60}$* in benzene. In both cases CR occurs through a spin-conserving process. Namely, the CR from the singlet charge-separated state to the $^3C_{60}$* in anisole takes place through the singlet−triplet mixing of the charge-separated state, whereas the CR from the singlet charge-separated state to the $^1C_{60}$* in benzene requires no singlet−triplet mixing of the charge-separated state. If the singlet−triplet mixing process in anisole is a rate-determining step, the slow rate of the mixing may be responsible for the slower CR rate from the charge-separated state to the $^3C_{60}$* in anisole, as compared with the CR rate to the $^1C_{60}$* in benzene. Such a difference in the CR rates would also result from the difference in the driving force. Overall, the energy level of the ZnP$^{\bullet+}$−$C_{60}^{\bullet-}$ in anisole becomes lower than the level in benzene, thereby being located between the enegy levels of $^1C_{60}$* (1.75 eV) and $^3C_{60}$* (1.50 eV). This is consistent with the fact that the fluorescence lifetimes of C_{60} (1100 ps) in ZnP−C_{60} in anisole is slightly shorter than that of C_{60}−ref (1300 ps) because of the slightly exergonic ET from ZnP to $^1C_{60}$* (k_{CS2} in Scheme 2). The k_{CS2} value and the quantum yield were determined as 1.4×10^8 s^{-1} and 0.15, respectively, on the basis of the fluorescence lifetimes (Table 2).

In benzonitrile ($\epsilon_s = 25.2$) as well, photoinduced ET takes place from ^{1}ZnP* to C_{60} in ZnP−C_{60} upon photoexcitation of the ZnP moiety, leading to the production of the charge-separated state with a rate constant of 9.5×10^9 s^{-1} and the quantum yield of 0.95 (Table 2). In addition, CS also occurs from ZnP to $^1C_{60}$* in ZnP−C_{60} upon photoexcitation of the C_{60} moiety to give rise to the charge-separated state with a rate constant of 5.5×10^8 s^{-1} and the quantum yield of 0.42. Complementary nanosecond experiments, performed with ZnP−C_{60}, also confirmed a characteristic absorption maximum of $C_{60}^{\bullet-}$ at 1010 nm, together with the broad absorption due to ZnP$^{\bullet+}$ around 650 and 850 nm (Figure 8a). The time profile of ZnP−C_{60} at 1010 nm reveals the rise and decay components with rate constants of 1.5×10^7 s^{-1} and 1.3×10^6 s^{-1}, respectively (Figure 8b). Judging from the energy level diagram

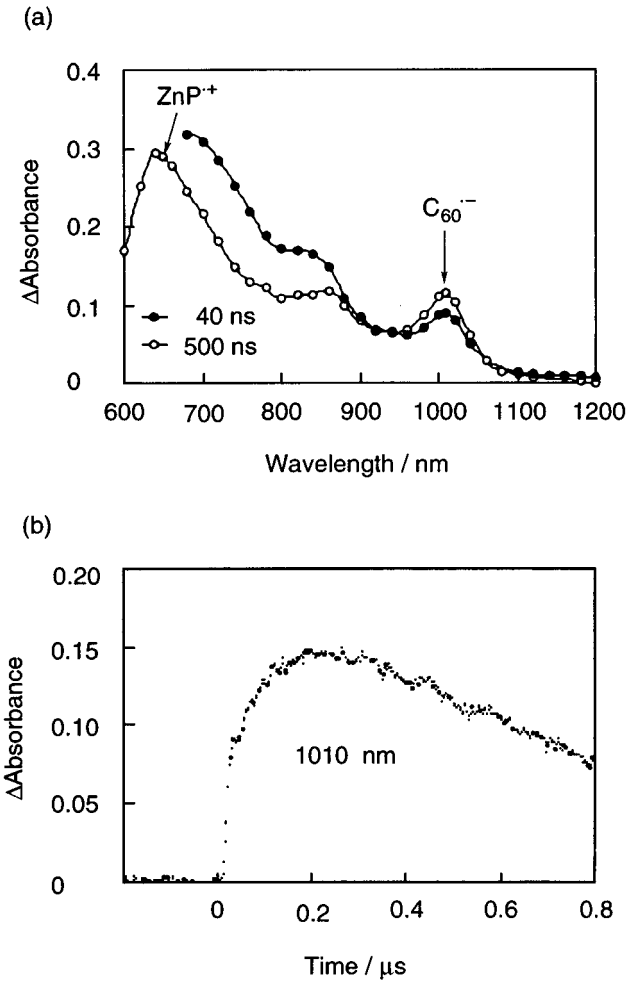

Figure 8. (a) Nanosecond time-resolved absorption spectra obtained by 532-nm (absorption ratio of ZnP:C_{60} = 77:23) laser photolysis of ZnP−C_{60} (0.1 mM) in argon-saturated benzonitrile and (b) time profiles of absorbance at 1010 nm.

SCHEME 3: Schematic Energy Levels and Relaxation Pathways for ^{1}ZnP* and $^1C_{60}$* in ZnP−C_{60} in Benzonitrile; $k_0 = 5.0 \times 10^8$ s^{-1}, $k_{CS1} = 9.5 \times 10^9$ s^{-1}, $k_{CS2} = 5.5 \times 10^8$ s^{-1}, $k_{CS3} = 1.5 \times 10^7$ s^{-1}, $k_{CR1} = 1.3 \times 10^6$ s^{-1}, $k_{ISC} = 7.7 \times 10^8$ s^{-1}, $k_T = 1.1 \times 10^5$ s^{-1}

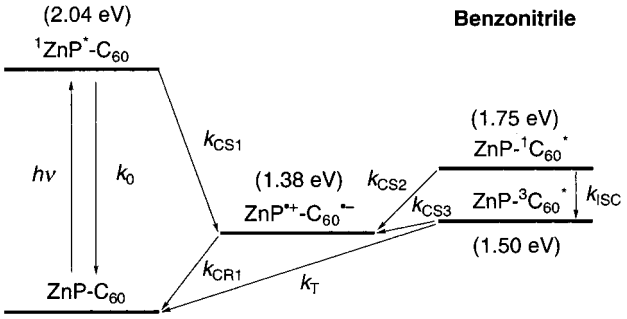

in benzonitrile (Scheme 3), photoinduced CS from ZnP to $^3C_{60}$* also takes place to yield the charge-separated state, which corresponds to the rise in absorbance at 1010 nm with a rate constant of 1.5×10^7 s^{-1}. Given the rate constant for the decay of $^3C_{60}$* in benzonitrile (1.1×10^5 s^{-1}), the quantum yield for formation of the charge-separated state from $^3C_{60}$* is 0.99 (Table 2). Accordingly, the photoinduced CS occurs from ^{1}ZnP*, $^1C_{60}$*, and $^3C_{60}$*, resulting in formation of the same charge-separated state with a total quantum yield of almost unity.[24] This is consistent with the quantum yield ($\Phi = 0.85$)[15] determined using the comparative method ($\epsilon_{1000\ nm} = 4700$ M^{-1} cm^{-1}).[25] The resulting charge-separated state recombines to regenerate the ground state with a rate constant of 1.3×10^6 s^{-1}, which is about four orders of magnitude smaller than the CS rate from ^{1}ZnP* (9.5×10^9 s^{-1}). This is in sharp contrast with conventional porphyrin−quinone dyads, where the CR rates are much faster than the CS rates in polar solvents.[1,21a−c] The accelerated CS and decelerated CR can be rationalized by the small reorganization energy of porphyrin−C_{60} dyads, as compared with those of conventional donor−acceptor linked systems.

In conclusion, solvent dependence of CS and CR processes in porphyrin−fullerene dyad has been well established in the present systems. In particular, solvent dependence of decay pathway from the charge-separated state to the excited states of C_{60} versus the ground state has been clarified in detail. The resulting ET dynamics can be rationalized by the small reorganization energy of porphyrin−fullerene systems. Such information will be helpful for understanding fundamental properties of ET on donor−acceptor systems and, in turn, developing artificial photosynthetic systems.

Acknowledgment. This work was supported by Grants-in-Aid for COE Research and Scientific Research on Priority Area of Electrochemistry of Ordered Interfaces and Creation of Delocalized Electronic Systems from Ministry of Education, Science, Sports and Culture, Japan. H.I. thanks the Sumitomo Foundation for financial support.

References and Notes

(1) (a) Wasielewski, M. R. *Chem. Rev.* **1992**, *92*, 435. (b) Gust, D.; Moore, T. A.; Moore, A. L. *Acc. Chem. Res.* **1993**, *26*, 198. (c) Paddon-Row, M. N. *Acc. Chem. Res.* **1994**, *27*, 18. (d) Osuka, A.; Mataga, N.; Okada, T. *Pure Appl. Chem.* **1997**, *69*, 797. (e) Blanco, M.-J.; Jiménez, M. C.; Chambron, J.-C.; Heitz, V.; Linke, M.; Sauvage, J.-P. *Chem. Soc. Rev.* **1999**, *28*, 293. (f) Verhoeven, J. W. In *Electron Transfer*; Jortner, J., Bixon, M., Eds.; John Wiley & Sons: New York, 1999; Part 1, pp 603−644.

(2) (a) *Anoxygenic Photosynthetic Bacteria*; Blankenship, R. E., Madigan, M. T., Bauer, C. E., Eds.; Kluwer Academic Publishers: Dordecht, 1995. (b) Moser, C. C.; Keske, J. M.; Warncke, K.; Farid, R. S.; Dutton, P. L. *Nature* **1992**, *355*, 796.

(3) (a) Marcus, R. A. *Annu. Rev. Phys. Chem.* **1964**, *15*, 155. (b) Marcus, R. A.; Sutin, N. *Biochim. Biophys. Acta* **1985**, *811*, 265. (c) Marcus, R. A. *Angew. Chem. Int. Ed. Engl.* **1993**, *32*, 1111.

(4) (a) Sariciftci, N. S. *Prog. Quant. Electr.* **1995**, *19*, 131. (b) Jensen, A. W.; Wilson, S. R.; Schuster, D. I. *Bioorg. Med. Chem.* **1996**, *4*, 767. (c) Gust, D.; Moore, T. A.; Moore, A. L. *Res. Chem. Intermed.* **1997**, *23*, 621. (d) Prato, M. *J. Mater. Chem.* **1997**, *7*, 1097. (e) Martín, N.; Sánchez, L.; Illescas, B.; Pérez, I. *Chem. Rev.* **1998**, *98*, 2527. (f) Diederich, F.; Gómez-López, M. *Chem. Soc. Rev.* **1999**, *28*, 263. (g) Sun, Y.-P.; Riggs, J. E.; Guo, Z.; Rollins, H. W. In *Optical and Electronic Properties of Fullerenes and Fullerene-Based Materials*; Shinar, J., Vardeny, Z. V., Kafafi, Z. H., Eds.; Marcel Dekker: New York, 2000, pp 43−81.

(5) (a) Imahori, H.; Hagiwara, K.; Akiyama, T.; Aoki, M.; Taniguchi, S.; Okada, T.; Shirakawa, M.; Sakata, Y. *Chem. Phys. Lett.* **1996**, *263*, 545. (b) Imahori, H.; Sakata, Y. *Adv. Mater*. **1997**, *9*, 537. (c) Imahori, H.; Sakata, Y. *Eur. J. Org. Chem.* **1999**, 2445. (d) Guldi, D. M. *Chem. Commun.* **2000**, 321. (e) Imahori, H.; Tamaki, K.; Yamada, H.; Yamada, K.; Sakata, Y.; Nishimura, Y.; Yamazaki, I.; Fujitsuka, M.; Ito, O. *Carbon* **2000**, *38*, 1599. (f) Tkachenko, N. V.; Guenther, C.; Imahori, H.; Tamaki, K.; Sakata, Y.; Fukuzumi, S.; Lemmetyinen, H. *Chem. Phys. Lett.* **2000**, *326*, 344. (g) Guldi, D. M.; Prato, M. *Acc. Chem. Res.* **2000**, *33*, 695.

(6) (a) Liddell, P. A.; Sumida, J. P.; Macpherson, A. N.; Noss, L.; Seely, G. R.; Clark, K. N.; Moore, A. L.; Moore, T. A.; Gust, D. *Photochem. Photobiol*. **1994**, *60*, 537. (b) Kuciauskas, D.; Lin, S.; Seely, G. R.; Moore, A. L.; Moore, T. A.; Gust, D.; Drovetskaya, T.; Reed, C. A.; Boyd, P. D. W. *J. Phys. Chem*. **1996**, *100*, 15926. (c) Liddell, P. A.; Kuciauskas, D.; Sumida, J. P.; Nash, B.; Nguyen, D.; Moore, A. L.; Moore, T. A.; Gust, D. *J. Am. Chem. Soc*. **1997**, *119*, 1400. (d) Kuciauskas, D.; Liddell, P. A.; Lin, S.; Johnson, T. E.; Weghorn, S. J.; Lindsey, J. S.; Moore, A. L.; Moore, T. A.; Gust, D. *J. Am. Chem. Soc*. **1999**, *121*, 8604. (e) Kuciauskas, D.; Liddell, P. A.; Lin, S.; Stone, S. G.; Moore, A. L.; Moore, T. A.; Gust, D. *J. Phys. Chem. B* **2000**, *104*, 4307.

(7) Bell, T. D. M.; Smith, T. A.; Ghiggino, K. P.; Ranasinghe, M. G.; Shephard, M. J.; Paddon-Row, M. N. *Chem. Phys. Lett*. **1997**, *268*, 223.

(8) (a) Baran, P. S.; Monaco, R. R.; Khan, A. U.; Schuster, D. I.; Wilson, S. R. *J. Am. Chem. Soc*. **1997**, *119*, 8363. (b) Cheng, P.; Wilson, S. R.; Schuster, D. I. *Chem. Commun*. **1999**, 89. (c) Schuster, D. I.; Cheng, P.; Wilson, S. R.; Prokhorenko, V.; Katterle, M.; Holzwarth, A. R.; Braslavsky, S. E.; Klihm, G.; Williams, R. M.; Luo, C. *J. Am. Chem. Soc*. **1999**, *121*, 11599.

(9) (a) Da Ros, T.; Prato, M.; Guldi, D. M.; Alessio, E.; Ruzzi, M.; Pasimeni, L. *Chem. Commun.* **1999**, 635. (b) Guldi, D. M.; Luo, C.; Prato, M.; Dietel, E.; Hirsch, A. *Chem. Commun*. **2000**, 373. (c) Guldi, D. M.; Luo, C.; Da Ros, T.; Prato, M.; Dietel, E.; Hirsch, A. *Chem. Commun.* **2000**, 375.

(10) (a) Nierengarten, J.-F.; Schall, C.; Nicoud, J.-F. *Angew. Chem. Int. Ed*. **1998**, *37*, 1934. (b) Armaroli, N.; Diederich, F.; Echegoyen, L.; Habicher, T.; Flamigni, L.; Marconi, G.; Nierengarten, J.-F. *New J. Chem*. **1999**, 77. (c) Armaroli, N.; Marconi, G.; Echegoyen, L.; Bourgeois, J.-P.; Diederlich, F. *Chem. Eur. J.* **2000**, *6*, 1629.

(11) Tkachenko, N. V.; Rantala, L.; Tauber, A. Y.; Helaja, J.; Hynninen, P. H.; Lemmetyinen, H. *J. Am. Chem. Soc*. **1999**, *121*, 9378.

(12) D′Souza, F.; Deviprasad, G. R.; Rahman, M. S.; Choi, J.-p. *Inorg. Chem.* **1999**, *38*, 2157.

(13) (a) Imahori, H.; Hagiwara, K.; Akiyama, T.; Taniguchi, S.; Okada, T.; Sakata, Y. *Chem. Lett.* **1995**, 265. (b) Imahori, H.; Sakata, Y. *Chem. Lett.* **1996**, 199. (c) Imahori, H.; Hagiwara, K.; Aoki, M.; Akiyama, T.; Taniguchi, S.; Okada, T.; Shirakawa, M.; Sakata, Y. *J. Am. Chem. Soc*. **1996**, *118*, 11771. (d) Sakata, Y.; Imahori, H.; Tsue, H.; Higashida, S.; Akiyama, T.; Yoshizawa, E.; Aoki, M.; Yamada, K.; Hagiwara, K.; Taniguchi, S.; Okada, T. *Pure Appl. Chem.* **1997**, *69*, 1951. (e) Tamaki, K.; Imahori, H.; Nishimura, Y.; Yamazaki, I.; Shimomura, A.; Okada, T.; Sakata, Y. *Chem. Lett.* **1999**, 227. (f) Imahori, H.; Ozawa, S.; Ushida, K.; Takahashi, M.; Azuma, T.; Ajavakom, A.; Akiyama, T.; Hasegawa, M.; Taniguchi, S.; Okada, T.; Sakata, Y. *Bull. Chem. Soc. Jpn*. **1999**, *72*, 485. (g) Yamada, K.; Imahori, H.; Nishimura, Y.; Yamazaki, I.; Sakata, Y. *Chem. Lett.* **1999**, 895.

(14) (a) Imahori, H.; Yamada, K.; Hasegawa, M.; Taniguchi, S.; Okada, T.; Sakata, Y. *Angew. Chem. Int. Ed. Engl.* **1997**, *36*, 2626. (b) Higashida, S.; Imahori, H.; Kaneda, T.; Sakata, Y. *Chem. Lett.* **1998**, 605. (c) Tamaki, K.; Imahori, H.; Nishimura, Y.; Yamazaki, I.; Sakata, Y. *Chem. Commun.* **1999**, 625. (d) Imahori, H.; Yamada, H.; Ozawa, S.; Ushida, K.; Sakata, Y. *Chem. Commun.* **1999**, 1165. (e) Fujitsuka, M.; Ito, O.; Imahori, H.; Yamada, K.; Yamada, H.; Sakata, Y. *Chem. Lett*. **1999**, 721. (f) Imahori, H.; Yamada, H.; Nishimura, Y.; Yamazaki, I.; Sakata, Y. *J. Phys. Chem. B* **2000**, *104*, 2099. (g) Imahori, H.; Norieda, H.; Yamada, H.; Nishimura, Y.; Yamazaki, I.; Sakata, Y.; Fukuzumi, S. *J. Am. Chem. Soc*. **2001**, *123*, 100.

(15) Luo, C.; Guldi, D. M.; Imahori, H.; Tamaki, K.; Sakata, Y. *J. Am. Chem. Soc*. **2000**, *122*, 6535.

(16) Prato, M.; Maggini, M. *Acc. Chem. Res.* **1998**, *31*, 519.

(17) Fujitsuka, M.; Watanabe, A.; Ito, O.; Yamamoto, K.; Funasaka, H. *J. Phys. Chem. A* **1997**, *101*, 7960.

(18) (a) Greaney, M. A.; Gorun, S. M. *J. Phys. Chem.* **1991**, *95*, 7142. (b) Dubois, D.; Kadish, K. M.; Flanagan, S.; Haufler, R. E.; Chibante, L. B. F.; Wilson, L. J. *J. Am. Chem. Soc.* **1991**, *113*, 4364. (c) Kato, T.; Kodama, T.; Shida, T.; Nakagawa, T.; Matsui, Y.; Suzuki, S.; Shiromaru, H.; Yamauchi, K.; Achiba, Y. *Chem. Phys. Lett.* **1991**, *180*, 446. (d) Gasyna, Z.; Andrews, L.; Schatz, P. *J. Phys. Chem.* **1992**, *96*, 1525.

(19) (a) Fuhrhop, J.-H.; Mauzerall, D. J. *J. Am. Chem. Soc.* **1969**, *91*, 4174. (b) Chosrowjan, H.; Taniguchi, S.; Okada, T.; Takagi, S.; Arai, T.; Tokumaru, K. *Chem. Phys. Lett.* **1995**, *242*, 644.

(20) Turro, N. J. *Modern Molecular Photochemistry*; The Benjamin/Cummings: Menlo Park, CA, 1978.

(21) (a) Wasielewski, M. R.; Niemczyk, M. P.; Svec, W. A.; Pewitt, E. B. *J. Am. Chem. Soc.* **1985**, *107*, 1080. (b) Asahi, T.; Ohkohchi, M.; Matsusaka, R.; Mataga, N.; Zhang, R. P.; Osuka, A.; Maruyama, K. *J. Am. Chem. Soc.* **1993**, *115*, 5665. (c) Macpherson, A. N.; Liddell, P. A.; Lin, S.; Noss, L.; Seely, G. R.; DeGraziano, J. M.; Moore, A. L.; Moore, T. A.; Gust, D. *J. Am. Chem. Soc.* **1995**, *117*, 7202. (d) Kroon, J.; Verhoeven, J. W.; Paddon-Row, M. N.; Oliver, A. M. *Angew. Chem. Int. Ed. Engl.* **1991**, *30*, 1358.

(22) Nojiri, T.; Watanabe, A.; Ito, O. *J. Phys. Chem. A* **1998**, *102*, 5215.

(23) Anderson, J. L.; An, Y.-Z.; Rubin, Y.; Foote, C. S. *J. Am. Chem. Soc.* **1994**, *116*, 9763.

(24) Because the energy level of ^{3}ZnP* (1.53 eV) is slightly higher than that of $^3C_{60}$* (1.50 eV), the charge-separated state may also be formed via ^{3}ZnP* through ET with a rate constant of $>1.5 \times 10^7$ s^{-1}. Considering the high quantum yield of formation of the ZnP triplet excited state (0.88) and C_{60} triplet excited state (0.98) and the slow decay rate constant (^{3}ZnP*: 2.3×10^4 s^{-1}; $^3C_{60}$*: 4.0×10^4 s^{-1}),[15] the total quantum yield of formation of the charge-separated state from ^{1}ZnP*, ^{3}ZnP*, $^1C_{60}$*, and $^3C_{60}$* in benzonitrile is estimated as almost unity [$\Phi = (0.95 + 0.05 \times 0.88) \times 0.77 + (0.42 + 0.58 \times 0.98 \times 0.99) \times 0.23 = 0.99$].

(25) Luo, C.; Fujitsuka, M.; Huang, C.-H.; Ito, O. *Phys. Chem. Chem. Phys.* **1999**, *1*, 2923.